INSTITUTE OF PHYSICS PUBLISHING JOURNAL OF PHYSICS: CONDENSED MATTER

J. Phys.: Condens. Matter **14** (2002) 6801–6813 PII: S0953-8984(02)30976-7

Raman scattering study of pressure-induced phase transitions in MIn_2S_4 spinels

V V Ursaki[1], F J Manjón[2,4], I M Tiginyanu[1,3] and V E Tezlevan[1]

[1] Institute of Applied Physics, Academy of Sciences of Moldova, 2028 Chisinau, Moldova
[2] Departament de Física Aplicada, Universitat Politècnica de València, EPSA, 03801 Alcoi, Spain
[3] Laboratory of Low-Dimensional Semiconductor Structures, Technical University of Moldova, 2004 Chisinau, Moldova

E-mail: fjmanjon@fis.upv.es

Received 8 April 2002, in final form 5 June 2002
Published 28 June 2002
Online at stacks.iop.org/JPhysCM/14/6801

Abstract

MIn_2S_4 (M = Mn, Cd, Mg) spinels were investigated by Raman scattering spectroscopy under hydrostatic pressure up to 20 GPa. These compounds were found to undergo a reversible phase transition to a Raman-inactive defect NaCl-type structure. Transition pressures of 7.2, 9.3, and 12 GPa were found for M = Mn, Cd, and Mg, respectively. From the analysis of the pressure behaviour of Raman-active modes, it was concluded that the phase transition from spinel to NaCl-type structure is direct in $MnIn_2S_4$ and $CdIn_2S_4$, while it occurs via an intermediate $LiVO_2$-type NaCl superstructure in $MgIn_2S_4$. The observed differences in pressure and path of the pressure-induced phase transition between these indium sulphide spinels are discussed.

1. Introduction

$A^{II}B_2^{III}C_4^{VI}$ compounds exhibit a variety of physical properties and some of them have proved to be promising for optoelectronics applications [1, 2]. Since these compounds can be grown in different crystalline structures, they are uniquely suited for use in investigating the role of structure and composition in the response of matter to external excitations such as heat, pressure, and electromagnetic fields. In view of this, systematic studies of the influence of hydrostatic pressure on the structure of tetrahedrally coordinated $A^{II}B_2^{III}C_4^{VI}$ [3–5] and $A^{I}B^{III}C_2^{VI}$ [6–9] compounds have been carried out during recent years. These studies have led to the observation of some important trends of pressure-induced phase transitions in zinc-blende-derived materials.

Most of the $A^{II}B_2^{III}C_4^{VI}$ compounds crystallize in the spinel structure. $A^{II}B_2^{III}C_4^{VI}$ spinels belong to the O_h^7 ($Fd3m$) space group with eight formula units per unit cell [10]. In this structure, the anions form a nearly ideal fcc framework surrounded by tetrahedral and

[4] Author to whom any correspondence should be addressed.

octahedral sites. Cations occupy only 1/8 of the tetrahedrally coordinated sites and 1/2 of the octahedrally coordinated sites. In an ideal spinel structure, A^{II} atoms are located on tetrahedral sites of T_d symmetry and B^{III} atoms on octahedral sites of D_{3d} symmetry; whereas C atoms occupy C_{3v} sites [10]. In real spinel structures, the distribution of the cations is not ideal, and the cations are sometimes disordered on their sites. The disordering of cations is described by means of the normality index, X. This parameter leads to a more general formula $A_XB_{1-X}(A_{1-X}B_{1+X})$ which describes the occupation of the tetrahedral (octahedral) positions in the lattice. The value of $X = 1$ describes an ideal spinel structure, while $X = 0$ corresponds to a inverse spinel structure. An ideal stochastic distribution is obtained with the value $X = 1/3$.

Investigations of spinels under pressure have important geophysical implications. The hypothesis of the layering of the Earth's mantle is mainly explained by the phase transitions of olivine-like compounds to the intermediate stage of spinel structure and finally to the perovskite-like structure as pressure and temperature increase with depth [11, 12]. Nevertheless, a limited number of high-pressure studies have been performed on $A^{II}B^{III}_2C^{VI}_4$ spinels up to now [13–16]. In this work, we investigate the common features in the behaviour of MIn_2S_4 spinels with different M cations and normality indices under hydrostatic pressure.

2. Experimental details

Spinel-type $MnIn_2S_4$, $CdIn_2S_4$, and $MgIn_2S_4$ single crystals were grown by chemical vapour transport using iodine as a transport agent [17]. For the optical measurements under pressure, the samples (100 μm $\times$ 100 μm in size and 30 μm thick) were inserted together with a ruby chip in a hole (250 μm in diameter) drilled in an Inconel gasket inside a Syassen–Holzapfel diamond anvil cell (DAC) with diamond culets 0.5 mm in diameter. Pressure was determined by calibration with the ruby luminescence [18], and a 4:1 methanol–ethanol mixture was used as pressure-transmitting medium ensuring hydrostatic conditions up to 10 GPa and quasi-hydrostatic conditions between 10 and 20 GPa [19]. Raman experiments at room temperature were performed in backscattering geometry using a Jobin-Yvon T64000 triple spectrometer in combination with a multi-channel CCD detector. The 647.1 nm line of a Kr^+-ion laser was used for excitation and the spectral resolution was of the order of 1 cm^{-1}. In order to avoid sample heating due to the focusing of the laser spot to a diameter of $\sim$50 μm, the excitation light power was kept below 5 mW at the entrance of the DAC.

3. Results and discussion

3.1. General considerations

The whole cubic cell of the spinel structure contains 56 atoms and is largely redundant as regards determining the number of vibrations of the lattice from group theoretical considerations since only two octants of the cell, which lie along the main body diagonal, are really different. Taking the reduced cell, which contains only 14 atoms and is equivalent to the smallest Bravais cell, the total number of vibration modes at the centre of the Brillouin zone, described by the irreducible representation of the O_h point group [20], is

$$\Gamma = A_{1g} + E_g + 3F_{2g} + 5F_{1u} + 2A_{2u} + 2E_u + F_{1g} + 2F_{2u}.$$

Five of these modes ($A_{1g}+E_g+3F_{2g}$) are Raman active, four F_{1u} modes are infrared active, and the remaining F_{1u} mode is an acoustic phonon. All other modes are silent. Figures 1(a), 2(a), and 3(a) show the Raman scattering (RS) spectra at different pressures of $MnIn_2S_4$, $CdIn_2S_4$, and $MgIn_2S_4$, respectively. The assignment of modes observed in the RS spectra, based on previous polarized measurements [21–23], is shown in table 1.

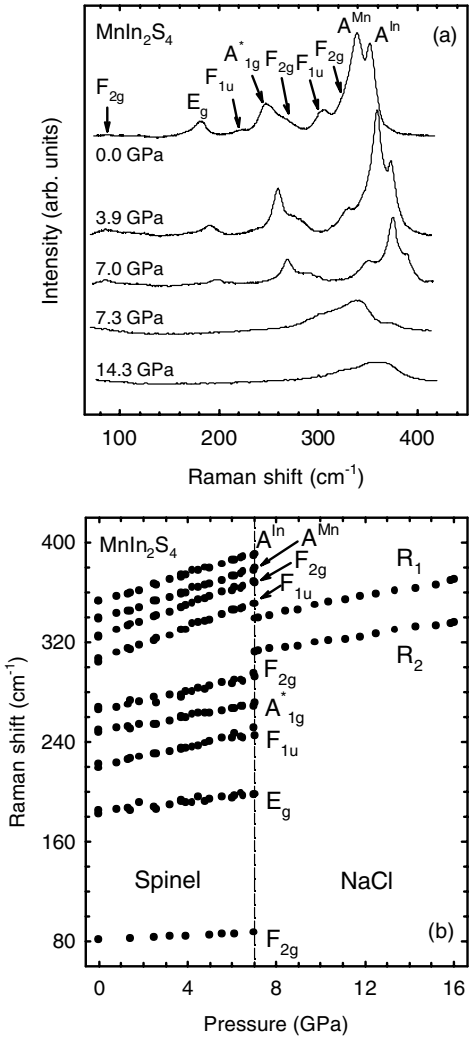

Figure 1. (a) Raman spectra of $MnIn_2S_4$ at various pressures. (b) Raman shifts as a function of pressure in $MnIn_2S_4$. The vertical dashed line indicates the pressure at which the phase transition between the spinel and the NaCl structures occurs. Error bars are not indicated for the sake of clarity.

A common feature of these spectra is the presence of some bands in addition to the Raman-active modes predicted by the space group analysis for an ideal spinel structure. According to polarized measurements [21, 22], the RS band in the region 230–260 cm^{-1} corresponds to a A_{1g} symmetry mode whose location is independent of sample composition. This band of A_{1g} symmetry, hereafter denoted as A^*_{1g}, was assumed to be a so-called clustering mode [21, 24] caused by a high density of states of a distinct phonon branch at $q \neq 0$. This mode is Raman allowed because of the increasing breakdown of the translation symmetry in partially inverse spinels due to the random distribution of the bivalent metals and indium on the octahedral sites. We must note, however, that Gupta and Balram [25] assumed in their theoretical analysis that this band corresponds to a E_g mode. It should also be noted that the emergence of some IR-active F_{1u} modes in the first-order RS spectra was explained by the same lowering in the

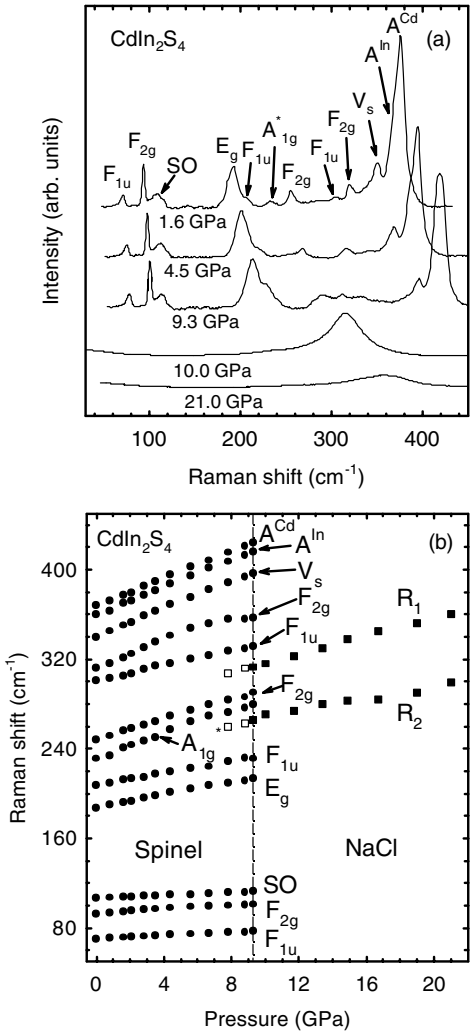

Figure 2. (a) Raman spectra of $CdIn_2S_4$ at various pressures. (b) Raman shifts as a function of pressure in $CdIn_2S_4$. The vertical dashed line indicates the pressure at which the phase transition between the spinel and the NaCl structures occurs. Error bars are not indicated for the sake of clarity.

symmetry caused by the disordering in the cation sublattice of partially inverse spinels [21, 23]. The frequencies of the F_{1u} modes in the Raman spectra correspond to those determined by IR reflectivity measurements [26–28]. Finally, other RS modes not expected are the modes SO and V_S in the spectra of $CdIn_2S_4$. We attribute these modes to second-order (SO) RS and local vibrations of the sulphur vacancies (V_S), respectively [23].

Another common feature of the spectra presented in figures 1(a), 2(a), and 3(a) is the non-elementary character of the high-energy A_{1g} mode consisting of two bands (see figure 4). It is well known that the A_{1g} breathing mode corresponds to the vibrations of the anions towards the centre of the tetrahedron [21]. Since in the partially inverse spinels, tetrahedra are occupied by both A and B atoms, the A_{1g} mode is formed by two bands, corresponding to the vibration of AS_4 and BS_4 tetrahedral units. The frequencies of the A_{1g} breathing modes

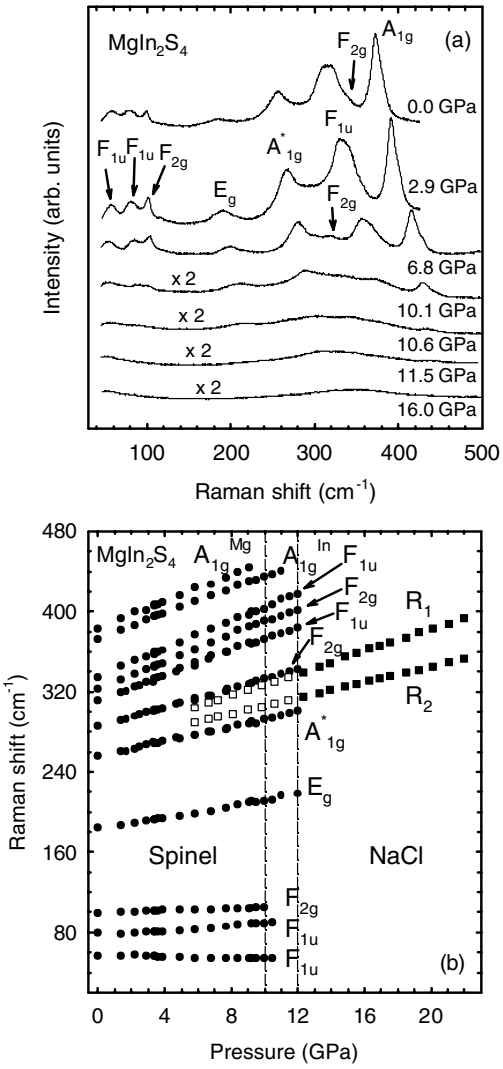

Figure 3. (a) Raman spectra of $MgIn_2S_4$ at various pressures. (b) Raman shifts as a function of pressure in $MgIn_2S_4$. The vertical dashed lines delimit the region where the $LiVO_2$-type NaCl superstructure is observed. Error bars are not indicated for the sake of clarity.

are almost unaffected by the masses of the metal ions involved, but are influenced by bonding and repulsion effects of the tetrahedrally coordinated metal ions [21]. Therefore, the phonon modes due to InS_4 vibrations are observed in all three compounds in the region 352–372 cm^{-1} (see figure 4). On the other hand, the A_{1g} mode corresponding to MS_4 vibrations (M = Mn, Cd, Mg), shows a larger shift for M = Mg, Cd than for M = Mn. This effect could be caused by the larger polarizability and covalency of Mg and Cd ions compared with those of Mn ions [21].

In order to analyse the experimental spectra, we have performed spectral decompositions of the Raman lines according to the previously discussed set of modes. Since the experimentally measured lineshapes result from the convolution of the Lorentzian profile of the Raman modes and the Gaussian profile given by the spectrometer resolution (1 cm^{-1}), we have fitted the spec-

Table 1. Zero-pressure frequencies (in cm^{-1}) and frequency–pressure coefficients (in cm^{-1} GPa^{-1}) of the Raman-active optical phonons in MIn_2S_4 spinels. Mode Grüneisen parameters γ calculated using a bulk modulus of $B_0 = 80$ GPa [32, 33] are also displayed. Typical errors in the determination of the parameters do not exceed 0.1 cm^{-1} for ω_0, 0.2 cm^{-1} GPa^{-1} for $d\omega/dP$, and 0.2 for γ.

Mode assignment	$MnIn_2S_4$			$CdIn_2S_4$			$MgIn_2S_4$		
	ω_0	$d\omega/dP$	γ	ω_0	$d\omega/dP$	γ	ω_0	$d\omega/dP$	γ
$F_{2g}(1)$	81	0.9	0.88	93	1.0	0.86	99	0.5	0.40
$F_{2g}(2)$	266	3.8	1.14	249	4.4	1.41	285	4.7	1.32
$F_{2g}(3)$	325	6.2	1.52	315	5.0	1.27	322	6.7	1.66
E_g	183	2.2	0.96	188	2.7	1.14	184	2.7	1.17
A_{1g}(In)	353	5.5	1.24	360	6.1	1.36	373	6.1	1.31
A_{1g}(M)	338	5.8	1.37	367	6.1	1.33	381	6.1	1.28
A^*_{1g}	247	3.2	1.04	232	5.2	1.79	256	3.6	1.13
$F_{1u}(1)$	—	—	—	70	0.7	0.80	57	−0.3	−0.4
$F_{1u}(2)$	—	—	—	—	—	—	77	1.1	1.14
$F_{1u}(3)$	221	4.0	1.45	207	2.6	1.00	311	6.1	1.57
$F_{1u}(4)$	306	6.5	1.70	301	3.3	0.88	335	6.8	1.62

tral lines to pseudo-Voigt functions. All spectral lines show a unique decomposition except for the close A_{1g} modes (see figures 4(b) and (c)). In this case we have taken the two mode frequencies as the mean values of those obtained after several fits with different initial parameters.

One of the methods of obtaining an estimation of the normality index of an spinel compound is provided by the relative Raman intensity of the $A_{1g}(MS_4)/A_{1g}(InS_4)$ bands which should be equal to $X/(1-X)$. On this basis, we have estimated the normality index in our spinels from the knowledge of the frequencies and intensities of the A_{1g} modes at different pressures. The attribution of the A_{1g} components to the In and M atoms is based on the following assumptions:

(i) the position of the InS_4 vibrations should not differ very much in different indium sulphide compounds [21]; and
(ii) the normality indices at ambient pressure are well known for these compounds from previous studies [28–31].

The mean position for the A_{1g} modes in these compounds is around 360 cm^{-1} at ambient pressure. The nearest peaks to this position are at 353, 360, and 373 cm^{-1} for $MnIn_2S_4$, $CdIn_2S_4$, and $MgIn_2S_4$, respectively. Therefore, it is reasonable to attribute these bands to the InS_4 vibrations, and to attribute correspondingly the bands at 338, 367, and 381 cm^{-1} to the MnS_4, CdS_4, and MgS_4 vibrations, respectively. The inverse attribution would lead to values of normality indices never observed in these compounds, which would strictly contradict the ambient pressure normality indices measured previously for these compounds from the x-ray diffraction data. The normality indices that we obtained are 0.16, 0.55, and 0.80 for $MgIn_2S_4$, $MnIn_2S_4$, and $CdIn_2S_4$, respectively. These values compare reasonably well with the normality indices previously reported for $MgIn_2S_4$(0.16) [28, 29], for $MnIn_2S_4$(0.66) [30], and for $CdIn_2S_4$ (between 0.50 and 0.80 depending on technological processing) [31].

The Raman shifts as a function of pressure for all the observed modes are shown in figures 1(b), 2(b), and 3(b) for $MnIn_2S_4$, $CdIn_2S_4$, and $MgIn_2S_4$, respectively. Error bars for the mode frequencies at different pressures are of the order of the scattering of the experimental points and have not been plotted in figures 1–3 for the sake of clarity. The mode frequencies in the spinel phase were found to increase linearly with pressure. Table 1 summarizes the

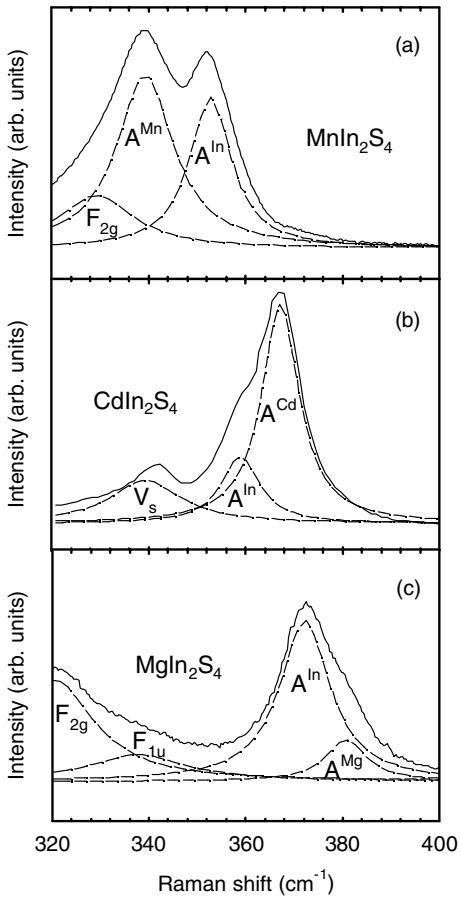

Figure 4. Spectral decomposition of the Raman spectra of $MnIn_2S_4$ (a), $CdIn_2S_4$ (b), and $MgIn_2S_4$ (c) at zero pressure in the vicinity of $A_{1g}(M^{II})$ and $A_{1g}(In^{III})$ modes.

values of the zero-pressure phonon frequencies (ω_0), pressure coefficients, and Grüneisen parameters $\gamma = (B_0/\omega_0)(\mathrm{d}\omega/\mathrm{d}P)$ in the spinel structure for the three compounds studied here. Errors in the determination of the parameters in table 1 from the least-squares fit do not exceed 0.1 cm^{-1} for ω_0, and 0.2 cm^{-1} GPa^{-1} for $\mathrm{d}\omega/\mathrm{d}P$, except for the F_{2g} mode in $CdIn_2S_4$, which deviates from a linear dependence at high pressures. For the estimation of the Grüneisen parameters of all modes in the different compounds, a bulk modulus $B_0 = 80$ GPa has been used for all crystals under consideration, as obtained from previous calculated and experimental values [32, 33].

3.2. Phase transition

It is well known that tetrahedrally coordinated $A^{II}B_2^{III}C_4^{VI}$ compounds undergo a phase transition to a Raman-inactive phase of disordered NaCl type under application of pressure [4]. On this basis, it has been shown that the spinel structure $CdIn_2Se_4$ compound transforms to NaCl-type structure or decomposes into CdSe and In_2Se_3 constituents at high pressure, depending on temperature [34]. MIn_2S_4 spinels are expected to behave in a similar way to defect chalcopyrites under pressure; i.e., a pressure-induced phase transition to a NaCl-type structure

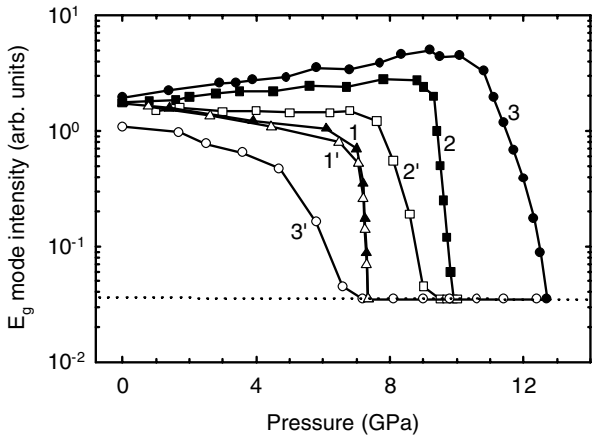

Figure 5. The pressure dependence of the intensity of the E_g mode in $MnIn_2S_4$ (curve 1, triangles), $CdIn_2S_4$ (curve 2, squares), and $MgIn_2S_4$ (curve 3, circles). Full symbols correspond to upstroke runs and open symbols to downstroke runs. The horizontal line indicates the sensitivity level of the experimental set-up.

is expected, despite x-ray diffraction analyses under pressure are necessary to prove this assumption. The transition to the NaCl phase in spinels is consistent with our observation of the disappearance of the Raman signal at pressures of 7.2, 9.3, and 12 GPa for M = Mn, Cd, and Mg, respectively (see figures 1(a), 2(a), and 3(a)) and the absence of a Raman signal from MS or M_2S_3 phases. The main difference between the spinels and tetrahedrally coordinated compounds is that the phase transition is reversible in spinels unlike in tetrahedrally coordinated compounds, as exemplified by the observation of the E_g mode of the spinel structure plotted in figure 5. Furthermore, the pressure at which the phase transition between the spinel and the NaCl-type structure occurs in MIn_2S_4 spinels seems to follow the same rules as were established for the zinc-blende-derived materials [4]. In this sense, it has been observed in these latter compounds that the lower the ionicity of the compound the higher the pressure of the phase transition. One example of this behaviour is shown by the family $AgGaS_2$, $AgGaSe_2$, $AgGaTe_2$ with average bond ionicities of 0.704, 0.709, and 0.712 and phase transition pressures of 15, 8.3, and 4.0 GPa, respectively [4].

According to Lutz *et al* [26], the ionicity of inverse spinels is smaller than that of ideal spinels. This means that the ionicity of $MnIn_2S_4$ and $CdIn_2S_4$ should be nearly the same as and higher than that of $MgIn_2S_4$ [26]. This result allows us to explain why the phase transition pressure in $MgIn_2S_4$ is higher than those of the other two compounds. On the other hand, since the normality index of $MnIn_2S_4$ increases with pressure and that of $CdIn_2S_4$ decreases (see figure 6(a)), one can expect the ionicity of $CdIn_2S_4$ to become lower than that of $MnIn_2S_4$. This result allows us also to explain why the phase transition pressure in $CdIn_2S_4$ is higher than that in $MnIn_2S_4$. Furthermore, the phase transition in spinels is characterized by a hysteresis cycle that seems to depend on the ionicity of the compound (see figure 5). In this sense, the phase transition in $MnIn_2S_4$ (highest ionicity) shows almost no hysteresis, while in $CdIn_2S_4$ and $MgIn_2S_4$ (lowest ionicity) the width of the hysteresis cycle is about 2 and 6 GPa, respectively. The averages of the critical pressures on compression and decompression in the centre of the hysteresis loop are 7.2, 8.6, and 9.0 GPa for $MnIn_2S_4$, $MgIn_2S_4$, and $CdIn_2S_4$, respectively.

In order to support our previous reasoning and despite the lack of knowledge of the bond ionicity values of our samples, we can estimate their relative bond ionicities in heterogeneous

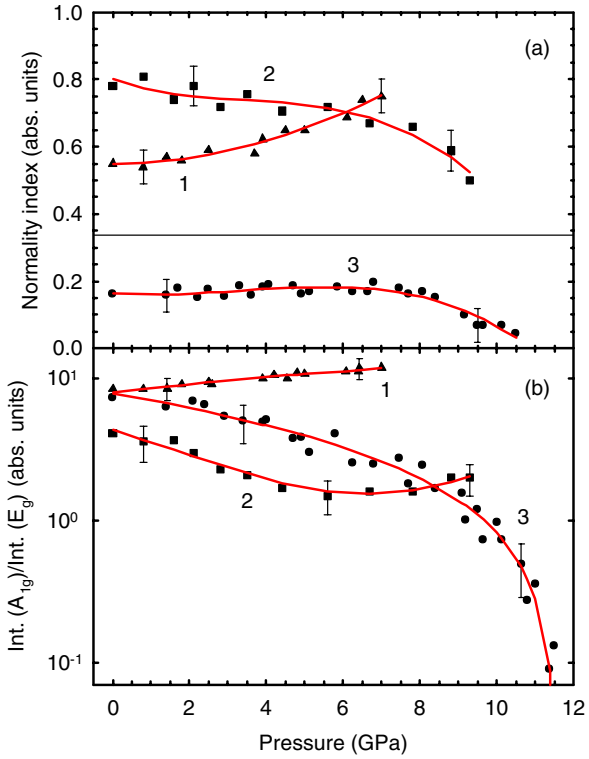

Figure 6. Pressure dependences of the normality index (a) and of the integral intensity of the A_{1g} mode normalized to the intensity of E_g mode (b) for $MnIn_2S_4$ (curve 1, triangles), $CdIn_2S_4$ (curve 2, squares), and $MgIn_2S_4$ (curve 3, circles). The curves are guides for the eye.

(This figure is in colour only in the electronic version)

compounds by studying the energy difference between the LO and TO RS modes. The higher the ionicity of the compound, the larger the LO–TO splitting. LO–TO splittings obtained from the analysis of $F_{1u}(3)$ and $F_{1u}(4)$ modes in FIR reflection spectra in several indium sulphide spinels are summarized in table 2 and compared with their phase transition pressures and normality indices at ambient pressure. A close agreement between the observed phase transition pressure on upstroke and the average ionicity of the compounds, as deduced from the LO–TO average splitting, is observed. On this basis, average LO–TO splittings below 35–40 cm^{-1} (low ionicity) seem to be related to almost inverse spinels with high phase transition pressures, whereas average LO–TO splittings above this range (high ionicity) seem to be related to almost normal spinels with lower phase transition pressures. We should note that the average ionicity of indium spinels has been estimated from the average of the $F_{1u}(3)$ modes (related to In vibrations in their octahedral sites) and the $F_{1u}(4)$ modes (mainly related to the S vibrations) because the two LO–TO values should be similar in all the indium sulphide spinels and their deviations could give an estimate of the ionicity of the compound. On the other hand, we should note that the ionicity of indium spinels cannot be obtained in the same way as that for defect chalcopyrites [4], because the ionicity of spinels is strongly affected by the degree of inversion. Otherwise, the ionicity of the $MgIn_2S_4$ would be higher than that of $CdIn_2S_4$ and $MnIn_2S_4$ according to the electronegativities of Mg (1.2), Cd (1.5), and Mn (1.6) [35]. However, despite these differences between spinels and defect chalcopyrites, the experimental phase transition

Table 2. Normality indices, LO–TO splittings, and cation M electronegativities and ion radii at ambient pressure for several indium sulphide spinels. Known pressures of phase transitions to the defect NaCl phase during upstroke are also reported.

Spinel compound	$NiIn_2S_4$	$MgIn_2S_4$	$CoIn_2S_4$	$CdIn_2S_4$	$HgIn_2S_4$	$MnIn_2S_4$
X (%)	0.10[a]	0.16[d,g]	0.17[a]	0.80[g], 0.50–0.80[e]	—	0.55[g], 0.66[a]
LO–TO (cm^{-1}) $F_{1u}(3)$ mode	25[b]	18[c]	31[f], 35[b]	56[b]	56[b]	49[b]
LO–TO (cm^{-1}) $F_{1u}(4)$ mode	28[b]	47[c]	27[f], 31[b]	32[b]	34[b]	40[b]
LO–TO average (cm^{-1})	26.5	32.5	29.0[f], 31.0[b]	44.0	45.0	44.5
Electronegativity (M ions)	1.8	1.2	1.7	1.5	1.5	1.6
Ion radius (M ions)	0.69	0.72	0.75	0.95	1.19	0.83
PT upstroke (GPa)	—	12.0[g]	—	9.3[g]	—	7.3[g]

[a] Reference [21].
[b] Reference [26].
[c] Reference [27].
[d] Reference [28, 29].
[e] Reference [31].
[f] Reference [36].
[g] This work.

pressure measured on upstroke of an almost ideal spinel structure such as $CdIn_2S_4$ can be well estimated according to rules established for tetrahedrally coordinated compounds [4]. In this context, figure 15 in [4] gives a correct estimation of the phase transition pressure in $CdIn_2S_4$ if we take into account the average ionicity value at ambient pressure (0.607) and the average cation–anion distance value at ambient pressure (2.504) reported in [4].

In spite of the common features of the phase transition to the defect NaCl phase in the three indium sulphide spinels studied, the characters of the transition are different for the three materials under consideration. This difference in character is indicated by the behaviour of the normality index as a function of pressure. Figure 6(a) presents the pressure dependence of the normality index as derived from the ratio $A_{1g}(MS_4)/A_{1g}(InS_4)$ of the intensities of two A_{1g} modes. The normality index of $MnIn_2S_4$ increases with pressure and approaches that of an ideal spinel structure. The normality index of $CdIn_2S_4$ decreases slowly with pressure and tends to the value 0.33 characteristic of a completely disordered structure. Finally, the normality index of $MgIn_2S_4$ is constant up to 9 GPa and decreases with further increase in pressure, thus indicating a tendency towards a totally inverse spinel structure. The decreasing normality index of $MgIn_2S_4$ is also confirmed by the increase of the overall intensity of the clustering A_{1g}^* mode [21]. This behaviour can be explained by the differences in cation radius and electronegativity between the M and In ions and the tendency of M ions to occupy a determined position in the lattice under pressure. For instance, the ion radius and electronegativity of Cd ions (0.95 and 1.5) are very close to those of In ions (0.80 and 1.5) [35]. As a result, they tend to occupy the tetrahedral and octahedral positions with the same probability with increasing pressure, leading to a stochastic distribution of cations. On the other hand, the ion radii and electronegativities of Mg (0.72 and 1.2) and Mn ions (0.83 and 1.6) lead to these ions which exhibit a tendency to occupy octahedral and tetrahedral positions, respectively, with increasing pressure. This behaviour suggests that in indium sulphide spinels the M ions with

larger electronegativity and ion radius than In have a natural tendency to occupy the tetrahedral positions, whereas those with smaller electronegativity and ion radius than In tend to occupy octahedral sites. This hypothesis seems to be supported by comparison of the normality indices and LO–TO splittings with ion radii and electronegativities in table 2. Inverse spinels have in common M-ion radii lower than that of In (0.80), while normal spinels show M-ion radii similar to that of In. If this tendency is correct and taking into account the similar electronegativities of Cr and In, one possible reason for the normal spinel structure of chromium sulphides and for the inverse spinel structure of indium sulphides [36] is the smaller ion radius of Cr (0.61) as compared to In (0.80). In this way, the low ionic radius of Cr prevents the formation of inverse spinels in chromium compounds, because M ions usually have larger ion radii.

Mn, Cd, and Mg indium sulphide spinel structures show different behaviours at the phase transition pressure. In $MnIn_2S_4$ and $CdIn_2S_4$ all Raman modes of the spinel structure disappear sharply at pressures of 7.2 and 9.3 GPa, respectively (see figures 1, 2, 5, and 6). In contrast, with increasing pressure above 10 GPa, the lowest-energy F_{2g} mode of $MgIn_2S_4$ disappears (see figure 1) and the A_{1g} mode intensity decreases sharply (see figure 6(b)). From these findings one can conclude that the number of tetrahedrally coordinated metal ions, which give rise to the A_{1g} breathing mode, diminishes with increasing pressure in $MgIn_2S_4$. This means that In atoms migrate from tetrahedral 8a sites to interstitial positions, i.e. to the normally unoccupied octahedral 16c sites. This migration leads to a phase transition to a NaCl superstructure with 1:1 ordering in the octahedral voids ($LiVO_2$ (cF64) type) [37]. In this structure, half of In ions occupy half of the octahedral 16c sites and the other half, together with Mg ions, locate at 16d sites ($LiVO_2$ defect structure). An analogous phase transition to a $LiVO_2$-type structure has also been reported in MLi_2Cl_4 inverse spinel-type compounds with increasing temperature [38].

Group theoretical considerations of the $LiVO_2$-type NaCl superstructure ($q \approx 0$) give the total number of vibration modes at the centre of the Brillouin zone. The result is Raman-active modes belonging to the irreducible representation $\Gamma = A_{1g} + E_g + 2F_{2g}$ [38]; i.e. one F_{2g} mode less than in spinel structure. This is consistent with the modes observed in figure 3(a).

With increasing pressure above 7.2, 9.3, and 12 GPa a phase transition to a defect NaCl structure occurs in $MnIn_2S_4$, $CdIn_2S_4$, and $MgIn_2S_4$ respectively. No RS peaks are expected in this structure; however, the Raman spectra of the three compounds above such pressures exhibit one broad band. This broad band has a non-elementary character and exhibits at least two maxima (marked as R1 and R2 in figures 1–3). This broad band is attributed to defect-induced first-order scattering due to the breakdown of the selection rules imposed by the non-translational symmetry along the crystal lattice after the phase transition. The maxima of the broad band are possibly related to maxima of the one-phonon density of states corresponding to the optical branch. Furthermore, we believe that these findings are indicative of the occurrence of a disordered NaCl structure with randomly distributed cations and vacancies in the octahedral sites, because similar features were observed in $MnLi_2Cl_4$ and $CdLi_2Cl_4$ compounds after a temperature-induced phase transition to a defect NaCl structure [38].

4. Conclusions

We have performed RS measurements on three indium thiospinels at room temperature up to 20 GPa. The pressure dependence of the frequency of the Raman modes in the spinel structure is reported and a phase transition probably to a disordered NaCl-type phase has been observed to occur at 7.2, 9.3, and 12 GPa in $MnIn_2S_4$, $CdIn_2S_4$, and $MgIn_2S_4$, respectively. This phase transition contrasts with that of spinels present in the Earth's mantle, which transform under pressure into a perovskite-like phase [11, 12], and with that of $MgAl_2O_4$ and $ZnAl_2S_4$ spinels, which undergo a phase transition to an amorphous [13, 16] or to a calcium ferrite-

type structure [14, 15]. $MnIn_2S_4$ and $CdIn_2S_4$ compounds, which show a nearly ideal spinel structure at zero pressure, transform directly into a disordered NaCl-type phase. On the other hand, $MgIn_2S_4$, which is almost an inverse spinel, do not transform directly from the spinel to the disordered NaCl type and this transition proceeds via an intermediate $LiVO_2$-type NaCl superstructure. This intermediate phase transforms into the disordered NaCl-type structure at higher pressures.

Despite the differences among the three compounds, they show several common features and follow similar trends.

(1) The phase transition pressure in the indium thiospinels studied follows similar trends to those of defect chalcopyrite materials [4]; i.e., the lower the ionicity of the compound, the higher the pressure of the phase transition to the defect NaCl phase.
(2) The differences in normality index of the three compounds at ambient pressure seem to be related to the different cationic radii and electronegativities of the M and In ions.
(3) The Raman spectra of the high-pressure defect NaCl structures in the three compounds are characterized by a similar non-elementary broad band attributed to disorder-induced first-order scattering.

Acknowledgments

The authors wish to express their gratitude to K Syassen at the Max Planck Institut für Festkörperforschung for his help in providing access to experimental set-ups and to W Dietrich, U Oelke and U Engelhardt for technical assistance in experiments. The authors also wish to thank to J González of the University of Los Andes (Venezuela) for a critical reading of the manuscript. VVU acknowledges financial support from the Deutscher Akademischer Austauschdienst and FJM acknowledges financial support from the European Union through a Marie Curie Fellowship under contract HPMF-CT-1999-00074.

References

[1] Radautsan S I and Tiginyanu I M 1993 *Japan. J. Appl. Phys. Suppl.* **32–3** 5
[2] See, for instance,
Tomlinson R D and Bullough W A (ed) 1998 *Proc. 11th Int. Conf. on Ternary and Multinary Compounds (Salford, UK, Sept. 1997) (Inst. Phys. Conf. Ser. 152)* (Bristol: Institute of Physics Publishing)
[3] Burlakov I I, Raptis Y S, Ursaki V V, Anastassakis E and Tiginyanu I M 1997 *Solid State Commun.* **101** 377
[4] Ursaki V V, Burlakov I I, Tiginyanu I M, Raptis Y S, Anastassakis E and Anedda A 1999 *Phys. Rev.* B **59** 257
[5] Ursaki V V, Burlakov I I, Tiginyanu I M, Raptis Y S, Anastassakis E and Anedda A 1998 *Proc. 11th Int. Conf. on Ternary and Multinary Compounds (Salford, UK, Sept. 1997) (Inst. Phys. Conf. Ser. 152)* (Bristol: Institute of Physics Publishing) p 605
[6] González J, Fernandez B J, Besson J M, Gauthier M and Polian A 1992 *Phys. Rev.* B **46** 15 092
[7] Tinoco T, Polian A, Itie J P, Moya E and González J 1995 *J. Phys. Chem. Solids* **56** 481
[8] González J, Calderon E, Tinoco T, Itie J P, Polian A and Moya E 1995 *J. Phys. Chem. Solids* **56** 507
[9] Tinoco T, Polian A, Gómez D and Itie J P 1996 *Phys. Status Solidi* b **198** 433
[10] Wyckoff R W G 1965 *Crystal Structures* vol 3, 2nd edn (New York: Interscience)
[11] Wood B J 1989 *Nature* **341** 278
[12] Ito E and Takahashi E 1989 *J. Geophys. Res.* B **94** 10 637
[13] Chopelas A and Hofmeister A M 1991 *Phys. Chem. Minerals* **18** 279
[14] Irifune T, Fujino K and Ohtani E 1991 *Nature* **349** 409
[15] Ursaki V V, Burlakov I I, Tiginyanu I M, Raptis Y S, Anastassakis E, Aksenov I and Sato K 1998 *Japan. J. Appl. Phys.* **37** 135
[16] Wittlinger J, Werner S and Schulz H 1998 *High Pressure Sci. Technol.* **7** 49
[17] Nitsche R 1971 *J. Cryst. Growth* **9** 238
[18] Piermarini G J, Block S, Barnett J D and Forman R A 1975 *J. Appl. Phys.* **46** 2774

[19] Piermarini G J, Block S and Barnett J D 1973 *J. Appl. Phys.* **44** 5377
[20] Unger W K, Farnworth B and Irwin J C 1978 *Solid State Commun.* **25** 913
[21] Lutz H D, Becker W, Muller B and Jung M 1989 *J. Raman Spectrosc.* **20** 99
[22] Anedda A, Berger G, Bongiovanni G and Mura A 1990 *Proc. 8th Int. Conf. on Ternary and Multinary Compounds (Kishinev, Sept. 1990)* ed S I Radautsan and C Schwab (Kishinev: Shtiintsa Press) p 301
[23] Gubanov V A, Kulikova O V, Kuliuk L L, Radautsan S I, Ratseev S A, Salivan G I, Tezlevan V E and Tsytsanu V I 1988 *Sov. Phys.–Solid State* **30** 258
[24] Fu Z-W and Dow J D 1987 *Phys. Rev.* B **36** 7625
[25] Gupta H C and Balram 1995 *J. Phys. Soc. Japan* **64** 142
[26] Lutz H D, Waschenbach G, Kliche G and Haeuseler H 1983 *J. Solid State Chem.* **48** 196
[27] Syrbu N N, Kretsu R and Tezlevan V E 1997 *Opt. Spectrosc.* **82** 247
[28] Wakaki M, Shintani O, Ogawa T and Arai T 1982 *Japan. J. Appl. Phys.* **21** 958
[29] Gastaldi L and Lapiccirella A 1979 *J. Solid State Chem.* **30** 223
[30] Lutz H D and Jung M 1988 *Z. Kristallogr.* **182** 177
[31] Burlakov I I, Ursaki V V, Tiginyanu I M and Radautsan S I 1998 *Proc. 11th Int. Conf. on Ternary and Multinary Compounds (Salford, UK, Sept. 1997) (Inst. Phys. Conf. Ser. 152)* (Bristol: Institute of Physics Publishing) p 601
[32] Yamada M, Shirai T, Yamamoto K and Yabe K 1980 *J. Phys. Soc. Japan* **48** 874
[33] Marinelli M, Baroni S and Meloni F 1988 *Phys. Rev.* B **38** 8258
[34] Range K-J, Becker W and Weiss A 1969 *Z. Naturf.* b **24** 1654
[35] Pauling L 1945 *The Nature of the Chemical Bond* (Ithaca, NY: Cornell University Press)
Allred A L and Rochow E G 1958 *J. Inorg. Nucl. Chem.* **5** 264
Allred A L and Rochow E G 1961 *J. Inorg. Nucl. Chem.* **17** 215
[36] Kringe C, Oft B, Schellenschläger V and Lutz H D 2001 *J. Mol. Struct.* **596** 25
[37] Chieh C, Chamberland B L and Wells A F 1981 *Acta Crystallogr.* B **37** 1813
[38] Wussow K, Haeuseler H, Kuske P, Schmidt W and Lutz H D 1989 *J. Solid State Chem.* **78** 117